

Er³⁺-activated sol-gel silica confined structures for photonic applications

A. Chiappini^{a,*}, C. Armellini^a, A. Chiasera^a, Y. Jestin^a, M. Ferrari^a, E. Moser^b, G. Nunzi Conti^{c,d}, S. Pelli^d, R. Retoux^e, G.C. Righini^{d,f}

^a CNR-IFN, Istituto di Fotonica e Nanotecnologie, CSMFO Group, 38050 Trento, Italy

^b Dipartimento di Fisica, Università di Trento CSMFO Group, 38050 Trento, Italy

^c Centro Fermi, Compendio del Viminale, 00184 Roma, Italy

^d Laboratorio Materiali e Dispositivi Fotonici, IFAC – CNR, 50019 Sesto Fiorentino, Italy

^e Laboratoire CRISMAT, UMR 6508, ENSICAEN, 6 Blvd., Marechal Juin, 14050 Caen, France

^f CNR, Department of Materials and Devices, 00185 Roma, Italy

ARTICLE INFO

Article history:

Available online 28 November 2008

PACS:

42.70.–a

42.70.Qs

78.55.–m

81.20.Fw

82.70.Dd

Keywords:

Opals

Photonic band gap

Diffraction

Erbium

Photoluminescence

Microspheres

ABSTRACT

Sol-gel processing was used to obtain two different kinds of confined structures for photonic applications: (i) Er³⁺-activated sol-gel silica derived spherical microresonators and (ii) Er³⁺-activated silica inverse opal. Optical and spectroscopic assessment, as well as morphological and structural characterization of the systems, were performed.

© 2008 Elsevier B.V. All rights reserved.

1. Introduction

During the last years, the spreading of optical networks toward the final customers has triggered the research in innovative materials and processes for the development of compact and integrated optical devices. The possibility of developing optical confined structures and fabricating nanostructured multi-component materials has opened new possibilities in the field of basic and applied physics in a vast variety of areas covering information communication technologies, health and biology, structural engineering, and environment monitoring systems.

In this scenario the optical amplifier is a key enabling technology for the achievement of high-speed and high-volume transmission required in current optical transmission systems [1,2]. Since the photoluminescence peak of Er is at a wavelength around

1.5 μm, just inside the so-called third window of fiber communication systems, erbium-activated glasses have become one of the key materials in active photonic systems.

The short-term deliverable is to develop appropriate systems to optimize the exploitation of luminescence properties of Erbium. Er³⁺-activated confined structures at different scales fabricated by the sol-gel route thus offer interesting and cheap solutions. The last decade has seen a remarkable increase in the experimental efforts to control and enhance emission properties of emitters by tailoring the dielectric surrounding the source. The aim of this paper is to highlight and discuss some advances in erbium-activated glass-based photonic systems, where suitable geometries and appropriate innovative materials will all the tailoring and enhancement of optical and spectroscopic properties. In particular, the following topics are presented:

- (i) Er³⁺-activated sol-gel silica derived spherical microresonators.
- (ii) Er³⁺-activated silica inverse opal.

* Corresponding author. Tel.: +39 0461881695; fax: +39 0461881696.
E-mail address: chiappini@science.unitn.it (A. Chiappini).

2. Experimental

2.1. Er³⁺-activated sol-gel silica derived spherical microresonators

Er³⁺-activated silica microspheres were made using the sol-gel route in acid catalysis. Tetraethylorthosilicate (TEOS, Aldrich, >99%), glacial acetic acid (Carlo-Erba, 99.9%), distilled water (resistivity >15 MΩ/cm) and erbium (III) chloride (ErCl₃, Aldrich, 99%) were used as reagents. Briefly, a solution with the molar ratio TEOS:CH₃COOH:H₂O of 1:4:4, plus 1 wt% ErCl₃ was stirred for 30 min at room temperature. After synthesis, the SiO₂ particles were separated from the solution by centrifuging and then washed with pure ethanol. Finally, the particles were dried at 80 °C overnight and subsequently heat-treated at 1100 °C for 30 min. Particle sizes were determined from SEM (JEOL-JSM 6300) micrographs and the surface quality was investigated by TEM (JEOL 2010) measurements.

Photoluminescence spectroscopy (PL), in the region of the ⁴I_{13/2} → ⁴I_{15/2} transition of Er³⁺ ions was performed using the 514.5 nm line of an Ar⁺ ion laser and the 980 nm line of a Ti:Sapphire laser as excitation sources. The luminescence was dispersed by a 320 mm single-grating monochromator with a resolution of 1 nm. The light was detected using a NIR photomultiplier tube and standard lock-in techniques. PL spectra were performed on single sphere. Decay curves were obtained by recording the signal with a digital oscilloscope.

2.2. Er³⁺-activated silica inverse opal

Er³⁺-activated silica inverse opals were synthesized by the sol-gel process as follows:

The opal templates were assembled using a commercially available monodispersed polystyrene (PS) microsphere colloidal suspension (Duke Company – 1 wt%) with an average diameter of 270 nm. The PS template was prepared using a vertical deposition technique detailed elsewhere [3,4]. The silicon substrate was placed in a vial with deionized water containing 0.036 wt% PS in suspension. The water was then slowly evaporated at 50 °C in an oven [5].

The silica sol activated by erbium ions (SsEi) was obtained after stirring a solution of the following precursors for 2 h at room temperature: 0.428cc Tetraethyl Orthosilicate (TEOS), 0.001cc HCl, 3.6cc Ethanol, 0.069cc H₂O and 1.68 mg ErCl₃. The SsEi was filtered using a syringe filter with a 0.2 μm pore size. The void spaces of the

opal template were then infiltrated by dropping ~10 μl of SeEi over the samples and were left to dry at room temperature.

The template was removed by heat-treatment: the samples were slowly heated to 450 °C (at 0.1 °C/min) and then left at this temperature for 30 min. Furthermore a rapid thermal annealing at 900 °C for 10 min was carried out in order to promote a more complete condensation densification of the structure and elimination of adsorbed water.

The microstructure of the Er³⁺-activated silica inverse opal was investigated by means of Scanning Electron Microscope (SEM) (JEOL-JSM 6300). Optical properties of the opal structures were investigated by reflectance measurements at different angles, using a double beam Varian spectrophotometer in the UV-visible region.

Photoluminescence spectroscopic measurements were performed using the same technique use to investigate the PL in the Er³⁺-activated sol-gel silica derived spherical microresonators.

3. Results and discussions

3.1. Er³⁺-activated sol-gel silica derived spherical microresonators

Fig. 1a shows a SEM image of Er³⁺-activated silica spheres after synthesis, while Fig. 1b reports a TEM image of the spheres obtained.

From Fig. 1a we can notice that we have produced particles of different diameters, ranging from 100 nm to ~100 μm. Fig. 1b shows the high quality of the surfaces of the spheres obtained. These silica spheres can be separated and selected as a function of the dimension and Fig. 2 shows a photo of a single Er³⁺-activated silica sphere of about 100 μm stuck on a silica tapered fiber by means of an optically transparent adhesive component.

Fig. 3 shows the PL spectra obtained upon excitation at 514.5 and at 980 nm on the single sphere shown in Fig. 2. The shape of the emission band in Fig. 3 is typical of Er³⁺ ions in silica glasses with a main emission peak at 1537 nm, a Stark structure at 1560 nm, [4,6] and a spectral bandwidth, measured at 3 dB from the maximum intensity, of 27 ± 2 nm. Moreover we can notice that the shape of the luminescence band is the same for both 514.5 and 980 nm excitations, indicating that no site-selection effect is present [7].

Fig. 4 reports the luminescence decay curve from the metastable level ⁴I_{13/2} of Er³⁺ in single a microsphere heat-treated at 1100 °C, obtained upon excitation at 980 nm.

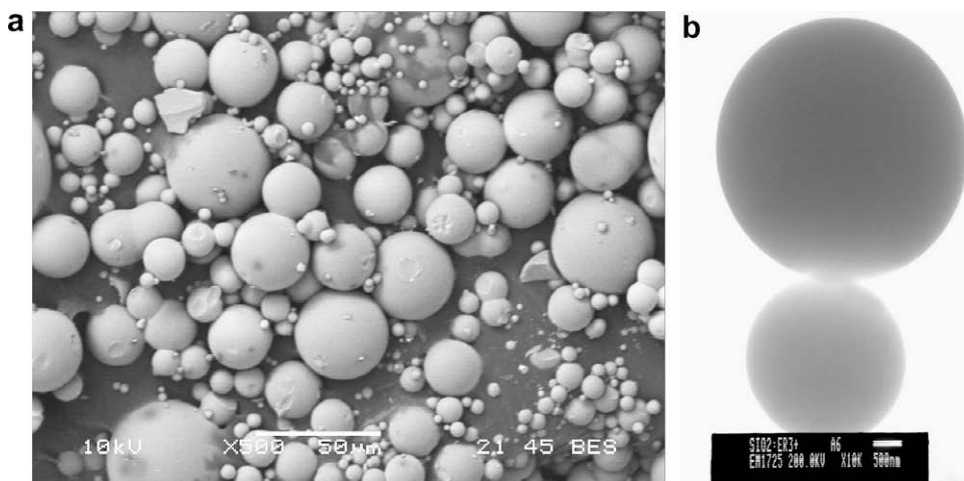


Fig. 1. (a) SEM image of Er³⁺ silica spheres obtained by sol-gel route in acid catalysis. (b) TEM image obtained for the spheres which indicates the high quality of the sphere surfaces.

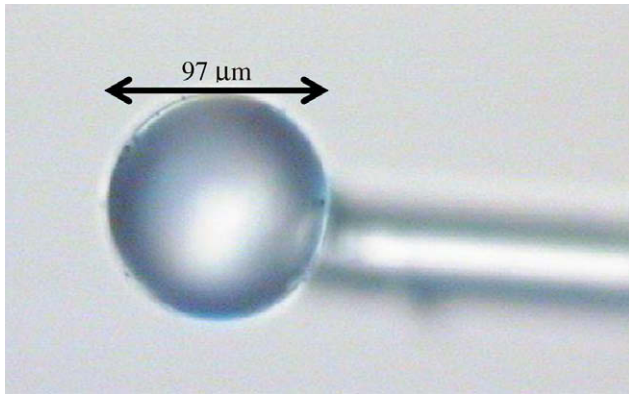


Fig. 2. Optical microphoto of a single Er^{3+} -activated silica sphere of about $100\ \mu\text{m}$ stuck on a silica tapered fiber by means a transparent optical component adhesive.

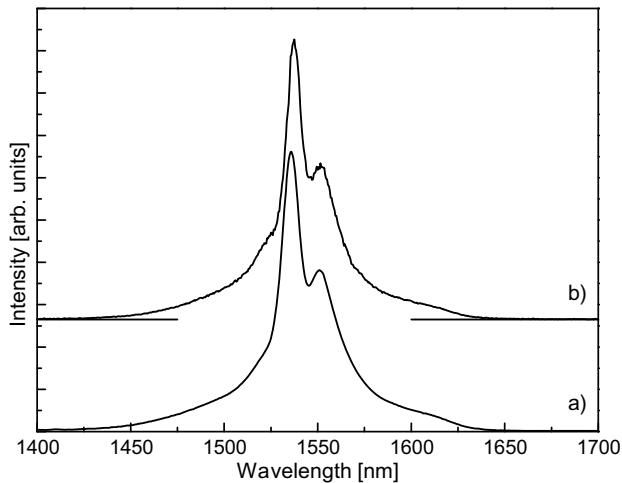


Fig. 3. PL spectra performed on a single sphere heat-treated at $1100\ ^\circ\text{C}$ upon excitation at: (a) $514.5\ \text{nm}$ and (b) $980\ \text{nm}$.

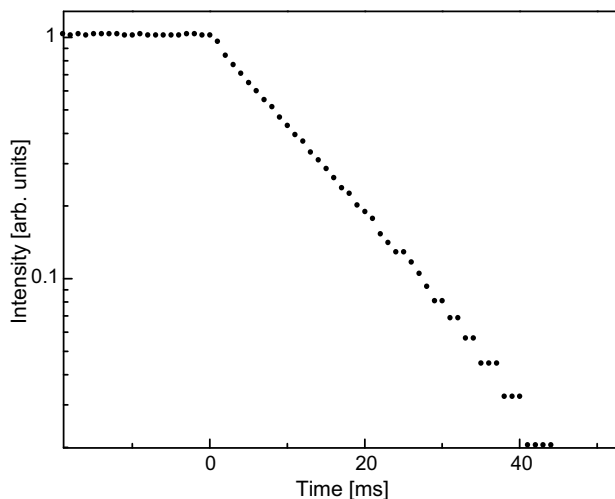


Fig. 4. Room temperature luminescence decay curve from the $4I_{13/2}$ state of Er^{3+} ions, obtained upon excitation at $980\ \text{nm}$, for a single sphere (Fig. 2) heat-treated at $1100\ ^\circ\text{C}$.

From Fig. 4 we can note that the decay curve exhibits a single exponential behavior, indicating that Er^{3+} ions all occupy sites characterized by similar local environment and a value of the measured lifetime $\tau_{\text{meas}} = 13.7 \pm 0.1\ \text{ms}$.

In order to obtain an estimate of the quantum efficiency η defined by the ratio: $\eta = \tau_{\text{meas}}/\tau_{\text{rad}}$ the measured lifetime (τ_{meas}) must be compared to the radiative lifetime τ_{rad} .

Recently, many investigations have been performed on SiO_2 spherical colloids doped with Er^{3+} ions, in order to study the spontaneous emission of the RE and to determine the local optical density (LOS) in these systems [8–10]. In particular, in these papers, a radiative lifetime of $18 \pm 3\ \text{ms}$ was determined, that is longer than lifetime found in several others studies of Er-doped silica-based glasses and structures [6,11]. Assuming this value of $18\ \text{ms}$ for τ_{rad} , a quantum efficiency η of 76% can be estimated for our microspheres heat-treated at $1100\ ^\circ\text{C}$. Due to the important incertitude of the radiative lifetime value the quantum efficiency incertitude is about 13%.

3.2. Er^{3+} -activated silica inverse opal

An SEM image of Er^{3+} -activated silica (ErSiO_2) inverse opals is shown in Fig. 5.

Fig. 5 reveals that the hollow regions of the air spheres are well ordered in a triangular lattice corresponding to the (111) planes of a fcc crystalline structure [12].

The average dimension of the air-hollows is $\sim 210\ \text{nm}$. This value is smaller than the diameter of the latex spheres ($270\ \text{nm}$) used to form the template, which demonstrates that a shrinkage occurs during the sintering process. This fact is not surprising given that the latex spheres are mesoporous and, in the early stages of calcination, probably decrease in size as water vapour is released from the pores [13,14].

The ErSiO_2 inverse opal sample exhibited violet regions, and the reflected light was easily observed by the naked eye, because the bright colour resulted from optical Bragg diffraction from the crystal planes.

Fig. 6 shows the normalized reflectance spectra obtained at different angles of ErSiO_2 inverse opals measured along the normal of the (111) plane of ErSiO_2 inverse opals.

From Fig. 6 we can observe that with an increase of the incident angle, the stop band position shifts to shorter wavelengths. This behavior can be express by modified form of Bragg's law:

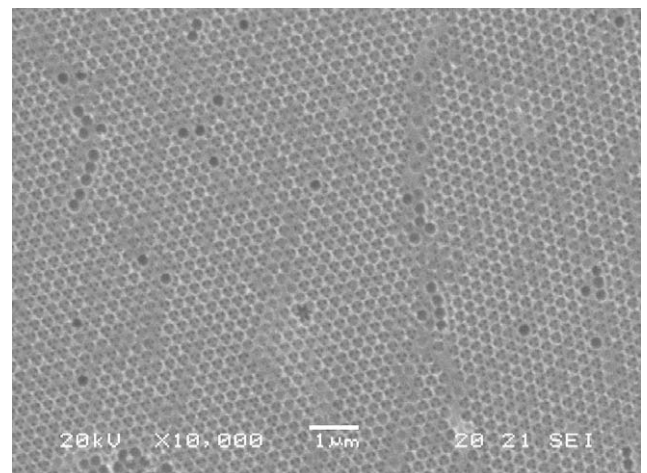


Fig. 5. Scanning Electron Microscopy image related to (111) facet of Er^{3+} -activated silica inverse opal.

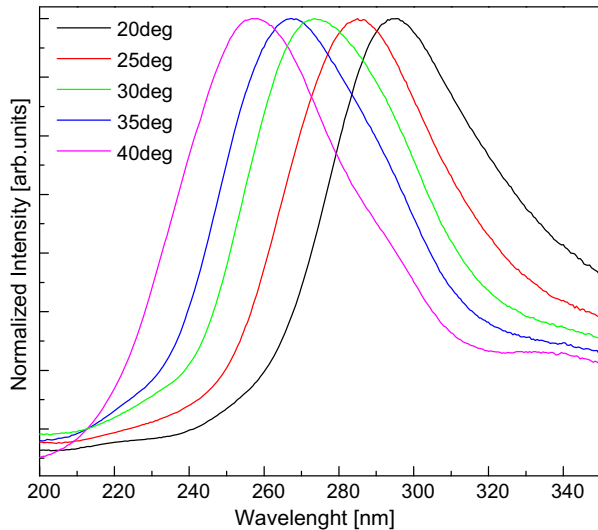


Fig. 6. Reflectance spectra at different incidence angles performed on the Er³⁺-activated silica inverse opal along the normal of the (1 1 1) plane of the sample.

$$\lambda = 2 \times 0.816 \times d \sqrt{(n_{\text{eff}})^2 - (\sin \theta)^2} \quad (1)$$

where λ is the free-space wavelength of light, d is the dimension size of the hollow spheres, n_{eff} is the effective refractive index and θ is the angle measured from the normal to the planes.

Moreover by using Eq. (1) and taking in count the following formula [4]:

$$n_{\text{eff}}^2 = n_{\text{air}}^2 \cdot f + n_{\text{silica}}^2 \cdot (1 - f) \quad (2)$$

It is possible to estimate the volume fraction of ErSiO₂ in the inverse opal sample.

In fact, assuming an effective refractive index of $n_{\text{eff}} = 1.1268$ (obtained, by fitting formula (1) with the incidence angles θ versus the stop band positions (free-space wavelength) λ) and considering the following values $n_{\text{silica}} = 1.4742$ and $n_{\text{air}} = 1$, we can calculate a volume fraction of about 23%, that it is very close to a maximal infiltration fraction for a inverse opal structure (26%). These results confirm the very good quality of the inverse structure obtained.

Fig. 7 shows the ⁴I_{13/2} → ⁴I_{15/2} PL spectrum of the ErSiO₂ inverse opal obtained upon excitation at 514 nm.

The PL of ErSiO₂ inverse opal exhibits a main emission peak at 1540 nm. The spectral width of the emission band measured at

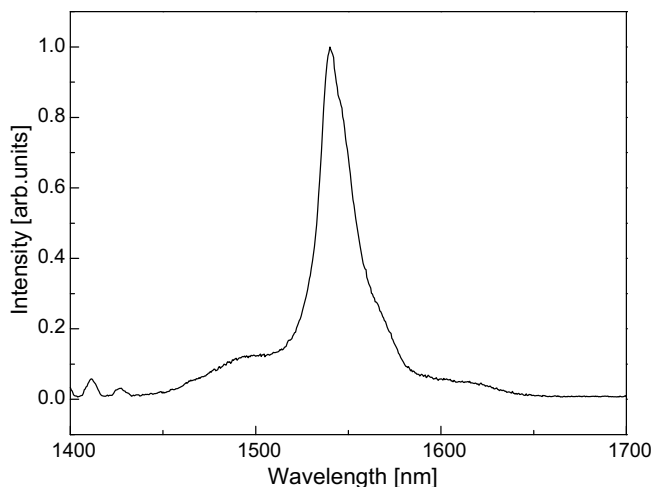


Fig. 7. Room temperature photoluminescence spectrum of ⁴I_{13/2} → ⁴I_{15/2}, transition of the Er³⁺ ions for the activated silica inverse opal, upon excitation at 514.5 nm.

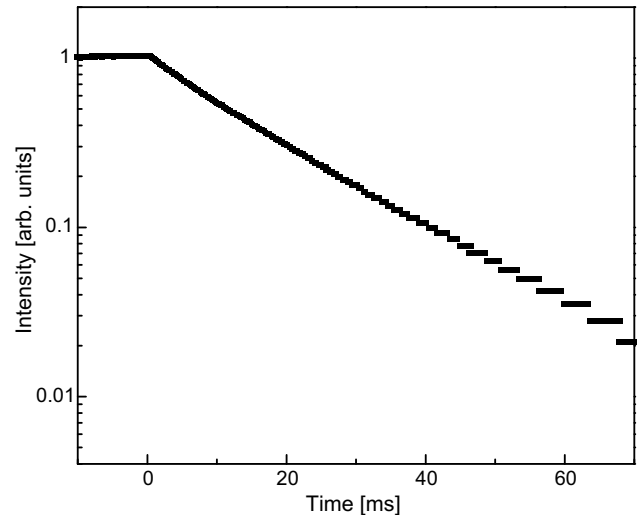


Fig. 8. Room temperature luminescence decay curve from the ⁴I_{13/2} state of E³⁺ ions for the activated silica inverse opal, heat-treated at 900 °C, upon excitation at 514.5 nm.

3 dB from the maximum of the intensity is 21 ± 1 nm, and the Stark structures at 1490, 1567 and 1617 nm appear well defined. This result indicates that Er³⁺ ions occupy sites characterized by similar local environment so that inhomogeneous broadening is not so important with respect to the amount of the Stark splitting [15].

Fig. 8 shows the room temperature luminescence decay curve from the ⁴I_{13/2} state of E³⁺ ions for the activated silica inverse opal, heat-treated at 900 °C, upon excitation at 514.5 nm.

Fitting the decay curve reported in Fig. 8, we obtain a lifetime $\tau_{1/e}$ of 16.8 ± 0.1 ms. This value indicates that the inverse opal structures present a very high quantum efficiency of the system.

4. Conclusions

In summary two different kinds of confined structures were fabricated using sol-gel routes.

A simple and a cheap protocol of synthesis was elaborated in order to obtain Er³⁺-activated microspheres suitable for microresonators. The protocol makes it possible to obtain Er³⁺-activated microspheres of different dimensions that possess a very high quality of the surfaces as revealed by TEM images. The PL spectra observed of a single sphere were typical of Er³⁺ ions imbedded in silica matrix. The decay curve of the metastable level ⁴I_{13/2} exhibits a single exponential profile with a lifetime τ_{meas} of 13.7 ± 0.1 ms for the spheres heat-treated at 1100 °C, and an estimated quantum efficiency of 76% for the system.

Er³⁺-activated silica (ErSiO₂) inverse opals were fabricated using colloidal route. Large and well ordered crystals of the inverse opal were pointed out by SEM images. Reflectance measurements showed the presence a pseudo photonic stop band in the visible regional. PL of ErSiO₂ inverse opal exhibits a main emission peak at 1540 nm, where the spectral width of the emission band measured at 3 dB from the maximum intensity is 21 ± 1 nm, and the Stark structures at 1490, 1567 and 1617 nm appear well defined. The decay curve of the ⁴I_{13/2} metastable state of the Er³⁺ ions presents a lifetime $\tau_{1/e}$ of 16.8 ± 0.1 ms corresponding to a very high quantum efficiency of the system.

Acknowledgements

Authors acknowledge the financial support of PAT FAPVU 2004–2006 and PAT FaStFAL (2007–2010).

References

- [1] E. Desurvire, Erbium-Doped Fiber Amplifiers, Principles and Applications, John Wiley, New York, 1994.
- [2] M.J.F. Digonnet, Rare-Earth-Doped Fiber Lasers and Amplifiers, Marcel Dekker Inc., 2001.
- [3] Y. Liu, X. Xu, D. Zhang, B. Cheng, D. Zhang, Appl. Phys. Lett. 86 (2005) 151102.
- [4] A. Chiappini, C. Armellini, S.N.B. Bhaktha, A. Chiasera, M. Ferrari, Y. Jestin, M. Mattarelli, M. Montagna, E. Moser, G. Nunzi Conti, S. Pelli, G.C. Righini, V.M. Sglavo, Proc. SPIE 182 (2006) 618223.
- [5] Y.-H. Ye, F. LeBlanc, A. Hache, V.-V. Truong, Appl. Phys. Lett. 78 (2001) 52.
- [6] W.J. Miniscalco, J. Lightwave Technol. 9 (1991) 234.
- [7] A. Chiasera, M. Montagna, C. Tosello, S. Pelli, G.C. Righini, M. Ferrari, L. Zampedri, A. Monteil, P. Lazzeri, Opt. Mater. 25 (2004) 117.
- [8] M.J.A. de Dood, L.H. Slooff, A. Polman, A. Moroz, A. van Blaaderen, Appl. Phys. Lett. 79 (2001) 3585.
- [9] L.H. Slooff, M.J.A. de Dood, A. van Blaaderen, A. Polman, Appl. Phys. Lett. 76 (2000) 3682.
- [10] M.J.A. de Dood, L.H. Slooff, A. Polman, A. Moroz, A. van Blaaderen, Phys. Rev. A 64 (2001) 0338071.
- [11] A.M. Vredenberg, N.E.J. Hunt, E.F. Schubert, D.C. Jacobson, J.M. Poate, G.J. Zydzik, Phys. Rev. Lett. 71 (1993) 517.
- [12] L.K. Teh, K.H. Yeo, C.C. Wong, Appl. Phys. Lett. 89 (2006) 051105.
- [13] B. Li, J. Zhou, R. Zong, M. Fu, L. Li, Q. Li, J. Am. Ceram. Soc. 89 (2006) 2308.
- [14] A. Richel, N.P. Johnson, D.W. McComb, Appl. Phys. Lett. 76 (2000) 1816.
- [15] S.N.B. Bhaktha, B. Boulard, S. Chaussedent, A. Chiappini, A. Chiasera, E. Duval, C. Duverger, S. Etienne, M. Ferrari, Y. Jestin, M. Mattarelli, M. Montagna, A. Monteil, E. Moser, H. Portales, K.C. Vishunubhatla, Opt. Mater. 28 (2006) 1325.